Arabian Journal of Chemistry (2020) 13, 1247–1258

King Saud University

Arabian Journal of Chemistry

www.ksu.edu.sa
www.sciencedirect.com

ORIGINAL ARTICLE

Effect of deashing on physico-chemical properties of wheat and rice straw biochars and potential sorption of pyrazosulfuron-ethyl

Suman Manna [a], **Neera Singh** [a,*], **T.J. Purakayastha** [b], **Anne E. Berns** [c]

[a] *Division of Agricultural Chemicals, ICAR-Indian Agricultural Research Institute, New Delhi 110012, India*
[b] *Division of Soil Science and Agricultural Chemistry, ICAR-Indian Agricultural Research Institute, New Delhi 110012, India*
[c] *Forschungszentrum Juelich GmbH, Institute of Bio- and Geosciences-Agrosphere (IBG-3), 52425 Juelich, Germany*

Received 10 August 2017; accepted 20 October 2017
Available online 31 October 2017

KEYWORDS

Pyrazosulfuron-ethyl;
Biochars;
Deashing;
Pyrolysis;
Sorption

Abstract Wheat (WBC) and rice straw biochars (RBC) prepared at 400 and 600 °C and their deashed counterparts were characterized for their physico-chemical properties using CHN analysis, Brunauer–Emmett–Teller (BET), X-ray fluorescence (XRF), scanning electron microscopy (SEM), ^{13}C-nuclear magnetic resonance (NMR), X-ray diffraction (XRD) and Fourier transform infrared (FT-IR) techniques. Pyrazosulfuron-ethyl sorption data on normal and deashed biochars could be well fitted to the Freundlich model. The characteristics of biochars and their adsorption capacities for pyrazosulfuron-ethyl were affected by the pyrolysis temperature and nature of feedstock. Rice biochars had higher sorption capacities than the wheat biochars. Deashing of biochars further enhanced their herbicide adsorption potential by a factor of 2–3. Sorption of herbicide on both normal and deashed biochars was concentration dependent ($1/n < 1$) and decreased with increase in the herbicide concentration in solution, indicating a saturation of sorption sites. The non-linearity of the isotherms increased with increasing pyrolysis temperature and deashing. Furthermore, adsorption of pyrazosulfuron-ethyl was affected by the pH, surface area and pore volume of biochars. Results of this study suggested that the mineral fraction of biochars significantly affected pyrazosulfuron-ethyl sorption.

1. Introduction

Biochar is the stable, recalcitrant carbonaceous material obtained after pyrolysis of biomass. The International Biochar Initiative Organization projected a conversion of nearly 80% of crop and forest residues into biochar and energy by 2050 (Kolodynska et al., 2012). Depending on the nature of feedstock and pyrolysis condition, the functional properties of

* Corresponding author.
E-mail address: drneerasingh@yahoo.com (N. Singh).
Peer review under responsibility of King Saud University.

Production and hosting by Elsevier

https://doi.org/10.1016/j.arabjc.2017.10.005
1878-5352

biochar vary significantly (Zhang et al., 2015; Mandal et al., 2017; Gamiz et al., 2017). Several studies suggested that high sorption potential of biochar for pesticides and organic pollutants (Wang et al., 2012; Zhang et al., 2013; Yu et al., 2016; Peng et al., 2017; Zhou et al., 2017a,b). Due to high organic carbon content, surface area and microporosity, biochar-amended soil was able to retain larger quantities of herbicide (Zhang et al., 2013; Cabrera et al., 2014) and ammonium nitrogen (Yang et al., 2015). Oxygenated functional groups mainly carboxylic, hydroxyl and phenolic groups present in biochar are effective in raising the cation exchange capacity of soil and its material retention capacity (Sohi et al., 2010). The composition of biomass significantly influenced the physico-chemical properties of biochars. Biomass materials mainly contain hemicelluloses, cellulose and lignin and their proportional abundance determines the extent of chemical, physical and structural changes of the biochars during processing (Mukome et al., 2013). The mineral components of biomass determine the extent of ash content of biochar. High ash contents can obstruct pores of biochar and consequently decrease its surface area and sorption capacity (Taha et al., 2014). Deashing of biochar resulted in a higher surface area and an increase of its sorption capacity for pesticides and organic pollutants (Sun et al., 2013; Taha et al., 2014; Yavari et al., 2015, Mandal et al., 2017).

Pyrolysis temperature (heat treatment temperature, HTT) too is an important factor influencing the sorption capacity of the resultant biochar (Yang et al., 2010; Rajapaksha et al., 2014). Increasing the pyrolysis temperature enhances the carbonized domain in biochar and results in an increase in competitive sorption (Cornelissen et al., 2005) rather than linear or non-competitive sorption in noncarbonized domain (Zhou et al., 2010). During pyrolysis the biochar undergoes physico-chemical transformations and depending on pyrolysis temperature four different states of chars are distinguished: transitional, amorphous, composite and turbostratic chars (Keiluweit et al. 2010). Chun et al. (2004) reported that sorption in low temperature (300–400 °C) chars occured through surface adsorption and partition into the residual organic matter phase while high temperature (400–700 °C) biochars showed surface adsorption on the carbonized surface. Low temperature biochars were highly effective in sorbing norflurazone and fluridone suggesting the importance of amorphous structure of aromatic moieties of these biochars (Sun et al., 2011).

Rice-wheat cropping system in India accounts for nearly 70% of the total cereal production. Jain et al. (2014) estimated that out of 620.43 million tonnes of field crop residues produced in India rice and wheat residues constituted approximately 53% and 33%, respectively. Out of nearly 120–150 million tonnes of surplus crop residues available in India, about 93 million tonnes are openly burned for land clearing. Thus, converting crop residues obtained during rice-wheat cultivation into biochars and incorporating them back in the same field will address the issue of land clearing, waste utilization and nutrient conservation (Yang et al., 2015; Pandian et al., 2016).

Pyrazosulfuron-ethyl (ethyl-5-(4,6-dimethoxypyrimidin- 2-yl-carbamoylsulfamoyl)-1-methylpyrazole-4-carboxylate) is a sulfonylurea herbicide, recommended for selective pre- and early post-emergence control of grassy and broad-leaved weeds in direct seeded and transplanted paddy cultivation. Major objective of the study was to investigate the effect of the biochar mineral fraction on pyrazosulfuron-ethyl sorption and to identify biochar properties affecting herbicide adsorption. Therefore, the present study reports the characterization of wheat and rice straw biochars (normal and deashed) and effect of their physico-chemical properties on sorption behavior of pyrazosulfuron-ethyl.

2. Materials and methods

2.1. Compounds

Analytical grade pyrazosulfuron-ethyl [purity: 98%, solubility in water = 9.76 mg L^{-1}; pK_a = 3.7; octanol-water partition coefficient, log P_{ow} = 1.3] was supplied by United Phosphorus Ltd (UPL), Mumbai, India. Chemicals and solvents used in the study were of analytical grade and were locally purchased.

2.2. Biochars

Biochars (BC) were prepared from the rice (*Oryza sativa*) and wheat (*Triticum aestivum*) straws. Briefly, straw was dried at 60 °C for 24 h to < 10% moisture and roughly chopped to 5 cm pieces. It was pyrolyzed in a muffle furnace equipped with digital temperature controller, tar trap, water cooling system and N_2 purge (1.5 mL min^{-1} flow rate) to ensure an oxygen-free atmosphere. The heating rate was 3 °C min^{-1} and residence time was 1 h at 400 or 600 °C. The respective wheat and rice biochars were named as WBC400, WBC600, RBC400 and RBC600.

To investigate the effect of the mineral components on pyrazosulfuron-ethyl sorption the biochars were demineralized using a mixture of 10% HF 1M HCl (v/v) (Sun et al., 2013). The deashed biochar samples prepared from WBC400, WBC600, RBC400 and RBC600 were named as WBC400d, WBC600d, RBC400d and RBC600d, respectively.

Both non-treated and deashed biochars were characterized for their physico-chemical properties *viz*., total organic carbon (TOC) content using carbon analyser (Elementar, Vario TOC Cube), elemental composition (C, H, N, O) analysis using EA3000 Elemental Analyser equipped with Callidus v.5.1 software, electrical conductivity, cation exchange capacity, dissolved organic carbon (DOC) by Walkley and Black method (Jackson, 1967). Specific surface area and pore volume were estimated using the BET nitrogen adsorption technique at 77 K in an automated manometric gas adsorption apparatus (Quantachrome NOVA 10.01, Quantachrome Instruments, Florida, USA). XRF analysis was carried out using a Philips PW 2404 X-ray spectrophotometer (WD-XRF) and XRD analyses were carried out using a Philips PW 1710 X-ray diffractometer using APD (Automated Powder Diffraction) software with the following setting: Cu-Kα radiation type, 40 kV generator voltage, 20 mA tube current, start angle (°2θ) – 3.00, end angle (°2θ) – 50.00, scan step size – 0.1, time per step – 4 s and type of scan - continuous. The FT-IR spectra were recorded in the range of 4000–400 cm^{-1} using KBr on a Bruker ALPHA FTIR system (typically 24 scans, resolution: 4 cm^{-1}). The scanning electron microscopy (SEM) images of the biochar samples were obtained on an EVO/MA10 microscope (CARL ZEISS Instrument, USA).

Solid-state ^{13}C-NMR spectra were obtained on a 7.05 T Varian INOVA™ Unity (Varian Inc., Palo Alto, CA, USA)

spectrometer operating at a ^{13}C resonance frequency of 75.4 MHz using the cross polarization magic angle spinning (CPMAS) pulse sequence.

2.3. Sorption studies

The sorption of pyrazosulfuron-ethyl in biochars, both non-treated (normal) and deashed, was studied using the batch method. Biochar (10 mg) and 10 mL 0.01M $CaCl_2$ aqueous solution of herbicide were shaken in 30 mL borosilicate stoppered glass tubes. The herbicide sorption was studied at five different concentrations ranging between 1.0 and 3.0 μg mL^{-1} and each concentration was replicated three times. Samples without herbicide served as controls. The samples were equilibrated at 25 ± 1 °C for 24 h, as preliminary studies indicated that equilibrium was attained after 24 h (results not shown). After equilibrium was attained, the samples were centrifuged at 3139*g* for 15 min and the herbicide concentration in the supernatant was quantified using high performance liquid chromatography (HPLC). The amount of contaminant sorbed was calculated from the difference between the initial and the final solution concentrations. The mass balance calculations indicated that the herbicide was stable during the 24 h of equilibration period and no sorption onto the glass surface was observed.

Desorption of the herbicide was studied in the same samples as used for the adsorption. After adsorption, the supernatant was decanted and was replaced with an equal volume of fresh 0.01 M $CaCl_2$ aqueous solution. The suspension was again shaken on an end-over-end shaker for 24 h and then centrifuged. The herbicide amount in the supernatant was determined by HPLC and the amount desorbed was calculated by subtracting the amount of herbicide in the entrapped solution after adsorption experiment from the solution concentration measured after the desorption experiment. Only one desorption step was performed for each sample.

2.4. Extraction and analysis

Aqueous samples were injected directly onto the HPLC column after filtration through 0.45. A reverse phase high performance liquid chromatography (HPLC) was used to quantify pyrazosulfuron-ethyl residue. A Varian Prostar instrument equipped with degasser, quaternary pump, UV detector connected to rheodyne injection system (20 μL loop) was used for analysis. The stationary phase consisted of Lichrospher C-18 packed stainless steel column (250 mm × 4 mm i.d). An isocratic elution with a mixture of acetonitrile:0.1% aqueous *o*-phosphoric acid (75:25) as mobile phase was set up at a flow rate of 0.5 mL min^{-1}. Under these conditions the retention time of pyrazosulfuron-ethyl was 7.5 min. Detection was performed at a wavelength of 234 nm. The recovery of pyrazosulfuron-ethyl from water samples was determined fortification levels of 0.01, 0.5 and 1 μg mL^{-1} by fortifying the 10 mL water samples with the required amount of herbicide in 0.1 mL of methanol. The pyrazosulfuron-ethyl recovery ranged from 92.8 ± 1.1% to 93.4 ± 1.0%.

3. Results and discussion

3.1. Biochar characterization

Physicochemical properties of biochars were affected by the nature of feed stock and the pyrolysis temperature (Table 1). The yield of wheat biochars (WBC400: 46.21%; WBC600: 40.78%) was larger than the rice biochars (RBC400: 36.03%; RBC600: 29.22%) and yield decreased with increase in the pyrolysis temperature. Non-deashed biochars were alkaline in nature (pH 9.3–11.1) and pH of rice biochars was higher than their respective wheat counterparts. Alkalinity increased with increase in pyrolysis temperature and was mainly attributed to higher metal oxides like Na_2O, K_2O and CaO content (Supplementary Table A) as ash content of biochars decreased with increase in pyrolysis temperature (Table 1). Deashing of biochars removed their alkaline mineral components; therefore deashed biochars were acidic in nature (3.2–4.1).

Total carbon content (TC) of both wheat and rice biochars, estimated by elemental analysis, increased with increase in pyrolysis temperature while nitrogen content showed a decline, indicating increased degree of carbonization in high temperature biochars. The TC content further increased following deashing as this procedure removed the mineral fraction.

Table 1 Physico-chemical properties of biochars.

Biochar	Yield [%]	pH	Ash (%)	TOC [%]	DOC [%]	CEC [$cmol_c$ kg^{-1}]	EC [dS m^{-1}]	C [%]	H [%]	N [%]	O [%]	H/C	O/C	SSA [m^2 g^{-1}]	Pore volume [cc g^{-1}]
WBC400	46.2	9.3	24.6	37.5	6.35	62.0	8.92	40.42	2.76	0.74	23.58	0.820	0.437	10.15	0.016
WBC600	40.8	10.4	22.5	40.5	6.20	62.6	10.39	42.98	1.54	0.61	8.97	0.430	0.156	20.38	0.026
RBC400	36.0	9.8	26.1	39.0	6.50	86.5	11.86	43.26	1.15	1.15	20.72	0.778	0.359	13.53	0.024
RBC600	29.2	11.1	24.1	41.7	6.21	45.3	14.27	46.07	0.94	0.94	9.24	0.480	0.150	12.60	0.034
WBC400d	ND	4.1	ND	66.7	ND	ND	ND	68.20	4.26	1.32	15.51	0.748	0.170	8.72	0.045
WBC600d	ND	4.1	ND	73.2	ND	ND	ND	75.32	2.53	1.06	6.95	0.403	0.069	51.91	0.083
RBC400d	ND	3.9	ND	67.9	ND	ND	ND	68.78	3.94	2.14	8.19	0.686	0.089	6.96	0.050
RBC600d	ND	3.2	ND	74.8	ND	ND	ND	79.65	2.64	1.99	7.46	0.397	0.070	126.69	0.371

TOC = Total organic carbon.
DOC = Dissolved organic carbon.
CEC = Cation exchange capacity.
EC = Electric conductivity.
SSA = Specific surface area.
ND = Not determined.

The O/C ratio was higher for biochars prepared at 400 °C than those prepared at 600 °C suggesting a higher polarity of low temperature biochars. The decrease in H/C ratio with increasing HTT suggested a higher degree of carbonization in high temperature biochars. There was no significant difference in the H/C ratio of wheat and rice biochars prepared at the respective temperatures, suggesting there may not be much difference in the aliphatic and aromatic carbon content of these biochars. Due to the removal of the oxide fraction following deashing, the carbon, nitrogen and hydrogen contents increased; however, H/C and O/C ratios decreased. This suggested that compared to normal biochars, the aromaticity increased while polarity decreased in deashed biochars. Total organic carbon (TOC) content of biochars prepared at 600 °C was higher than those prepared at 400 °C and deashing further increased the percent TOC content.

The surface area of wheat biochars doubled with increasing pyrolysis temperature, while it was nearly the same for both rice biochars (RBC400 and RBC600). However, pore volume of both wheat and rice biochars increased with increasing pyrolysis temperature and rice biochars had higher pore volume than wheat biochars. Earlier reports suggested that along with pyrolysis temperature and heating rate, the nature of biomass affected surface area and pore volume of biochars (Mandal et al., 2017). Deashing decreased the BET N_2 surface area of biochars prepared at 400 °C, but surface areas of biochars prepared at 600 °C showed a 2.5 and 10 times increase for wheat and rice biochars, respectively. A similar trend was observed for the pore volume. Taha et al. (2014) observed similar results for phosphoric acid treated biochars and suggested that an increase in functional groups inside the pores might have contributed to decreased surface area and pore volume.

XRF analysis suggested that all biochars contained significant fractions of Si-, Al- and K-oxides (Supplementary Table A). Rice biochars had higher silica contents while wheat biochars had higher iron contents. The SEM images (Supplementary Figure A) showed that original cell wall structure in biochar was intact and they were highly porous in nature. The evaluation results of the EDX spectra of biochars, showing surface elemental compositions, are shown in Supplementary Table B. These results clearly suggested that surface carbon contents of WBC600 and RBC600 were higher than those of WBC400 and RBC400. The EDX spectra also suggested the presence of silicon as the major element while aluminum, iron, potassium, calcium, magnesium, etc were present in smaller amounts.

The ^{13}C-NMR spectra (Fig. 1) showed no differences in the carbon structures between biochars prepared from different feed stocks at the same temperature. However, biochars prepared at different temperatures did not have identical NMR spectra. All NMR spectra had one main signal centered at 130 ppm in the aromatic region. The spectra of the biochars produced at 600 °C only had a hint of a shoulder at 140 ppm indicating some O-containing groups. The NMR spectra of the 400 °C biochars had a clear signal at 152 ppm stemming from O-substituted aromatic structures. These biochars in addition had aliphatic signals centered at 30 ppm. Neither of the biochars contained protein or carbohydrate structures. The relative structural carbon percentage (RSCP) (Supplementary Table C) showed that 400 °C biochars respectively

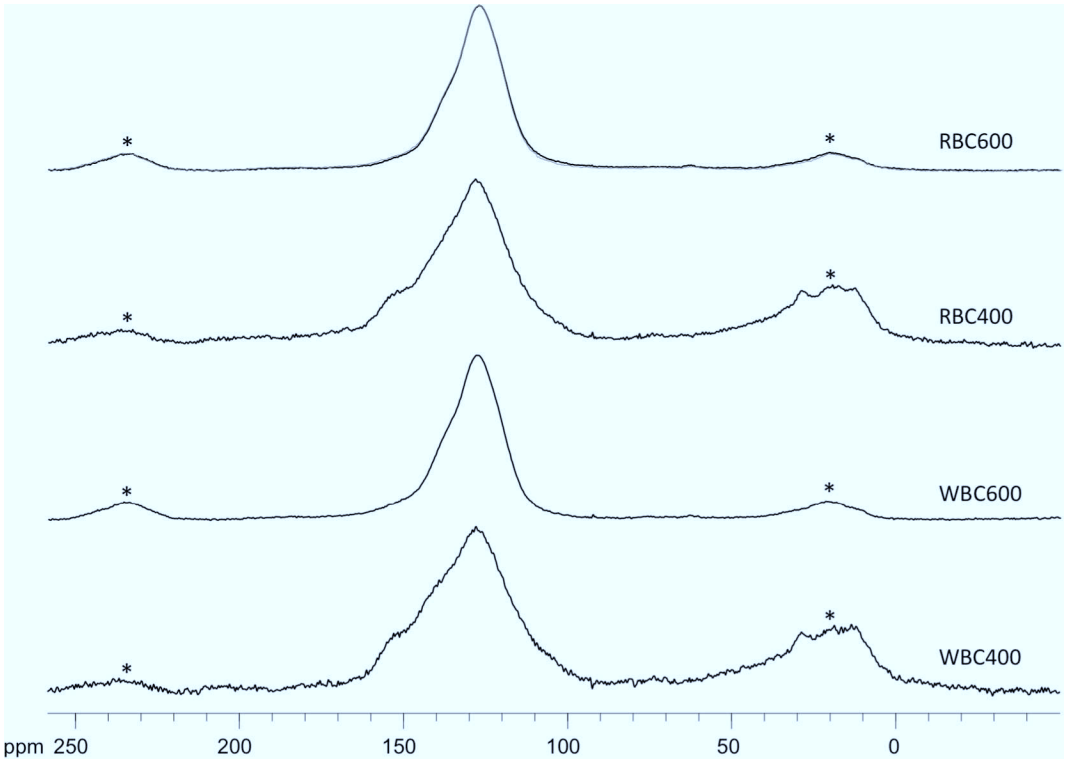

Fig. 1 ^{13}C NMR spectra of biochars (* = spinning side bands of aromatic region).

contained 25 and 75% of aliphatic and aromatic carbon structures while 600 °C biochars mainly composed of aromatic structures with only a few O-containing groups. The NMR spectra were well in line with the observed H/C and O/C contents and their respective positioning in the van Krevelen plot.

The XRD patterns of wheat and rice biochars (Supplementary Figure B) suggested the presence of inorganic minerals like SiO_2 (quartz, 2θ = 20.74°, 26.58°), KCl (sylvite, 2θ = 28.32°, 40.51°) and $CaCO_3$ (calcite, 2θ = 29.37°, 50.2°). The calcite ($CaCO_3$) peaks intensified when pyrolysis temperature was increased from 400° to 600 °C, indicating an increase in calcite content in high temperature biochars. Deashed biochar showed a diffused diffractogram (Supplementary Figure C) and majority of the peak disappeared due to loss of mineral following acid treatments. A broad peak at 2θ = 22–27° indicated the presence of amorphous silica while calcite peaks were observed in WBC600d.

The FTIR spectra of normal biochars (Supplementary Figure D) suggested, compared to feedstocks (spectra not shown), loss of aliphatic C—H stretching (2925 and 2850 cm^{-1}) and C—O stretching (1110–1030 cm^{-1}), indicating that feedstock underwent progressive dehydration and depolymerization. With increase in pyrolysis temperature (400–600 °C) the C—H stretching band (2925–2850 cm^{-1}) lost intensity, both in wheat and rice straw derived biochars. This implied greater dehydration and increased aromatization with increase in temperature (Pastorova et al., 1994). All normal biochars showed two characteristic bands in the region 1600–1630 cm^{-1} and 3200–3400 cm^{-1}, indicating C—C stretching of aromatic components and O—H stretching of hydroxyl groups, respectively (Liu et al., 2015). Presence of silicate structure was confirmed by the characteristic small band in the region 900–1050 cm^{-1} and XRF and XRD results also confirmed these finding. Cellulose-derived transformation products were reflected at 1440 (aromatic C—C skeletal vibrations) and 1375 cm^{-1} (C—H deformation in alkenes) (Pastorova et al., 1994). The relative intensities of the signals changed depending on the pyrolysis temperatures. The intensity of the O—H band at 3430 cm^{-1} slightly decreased as the pyrolysis temperature increased from 400–600 °C. This was attributed to progressive condensation and polymerization leading to loss of water molecules. The relative intensity of the C—C band at 1630 cm^{-1} also decreased as the charring temperature increased to 600 °C leading to formation of more condensed aromatic structures (tannins and lignin type). The FTIR spectra of deashed biochars (Supplementary Figure E) showed all characteristic peaks observed in normal biochar, but spectra were less cluttered than the normal biochar spectra and few new peaks were visible. The O—H stretching vibration peak at 3423–3438 cm^{-1} was not very sharp in deashed biochars. A characteristic band at 3043 cm^{-1} (N—H stretching of amine condensed with sugar components) became visible only after deashing of biochars. Similarly, peaks at 1700 cm^{-1} (C—O stretching vibrations), 1578–1559 cm^{-1} (aromatic C—C stretching vibration) 1459–1436 cm^{-1} (aromatic skeletal vibration combined with C—H in plane deformation or asymmetric C—O stretching vibration) 1266–1270 cm^{-1} (C—N stretching of aliphatic amine), 1212 cm^{-1} (C—O stretching vibration or OH plane deformation) were clearly visible only in deashed biochars (Wu et al., 2012).

3.2. Sorption studies

Table 2 shows the pyrazosulfuron-ethyl sorption parameters of normal and deashed biochars. The results suggested that biochars prepared at 600 °C had higher sorption capacities for pyrazosulfuron-ethyl (rice: 56.2–65.8%; wheat: 31.8–47.3%) than those prepared at 400 °C (rice: 19.2–23.2%; wheat: 8.6–9.7%) and rice straw biochars were more effective than their wheat counterparts. This is in line with earlier reports which suggested that the type of feedstock and production temperature affects the contaminant sorption potential of biochars (Sun et al., 2013). Deashing significantly enhanced pyrazosulfuron-ethyl sorption potential of biochars and 2–3 times increase in pyrazosulfuron-ethyl sorption was observed. Taha et al. (2014) reported that deashed biochars showed higher sorption capacities for 15 pesticides than their normal counterparts. Similarly, Sun et al. (2013) suggested that Koc values of phenanthrene on biochars increased after deashing and this was attributed to enhancement of hydrophobic sorption sites following the mineral fraction removal.

Data for pyrazosulfuron-ethyl sorption (Fig. 2) on normal and deashed biochars was subjected to the linear form of Freundlich adsorption isotherm:

$$\log\ C_s = \log\ K_f + 1/n\ \log\ C_e$$

C_s is the amount of herbicide adsorbed at equilibrium (μg g^{-1}), C_e is the equilibrium concentration of herbicide (μg mL^{-1}), and K_f and 1/n are sorption related constants calculated by regression analysis. The Freundlich constant K_f (intercept) represents the amount of contaminant adsorbed at an equilibrium concentration of 1 μg mL^{-1}. The constant 1/n (slope) is the measure of the intensity of sorption and reflects the degree to which sorption is the function of contaminant concentration. The correlation coefficients for all biochars were very high ($R > 0.96$), indicating that the Freundlich

Table 2 Freundlich parameters for pyrazosulfuron-ethyl adsorption in biochars.

Treatment	K_f	1/n	r	% Amount sorbed	K_{OC}
WBC400	101.5	0.93	0.995	8.6–9.7	270.6
WBC600	601.2	0.61	0.956	31.8–47.3	1484.4
RBC400	280.3	0.82	0.985	19.2–23.2	718.7
RBC600	1317.3	0.74	0.967	56.2–65.8	3288.5
WBC400d	294.7	0.57	0.966	17.6–26.1	485.4
WBC600d	1137.1	0.46	0.966	50.2–67.7	1553.4
RBC400d	758.0	0.39	0.969	32.9–56.1	1084.4
RBC600d	4227.7	0.52	0.966	86.0–93.6	5652.0

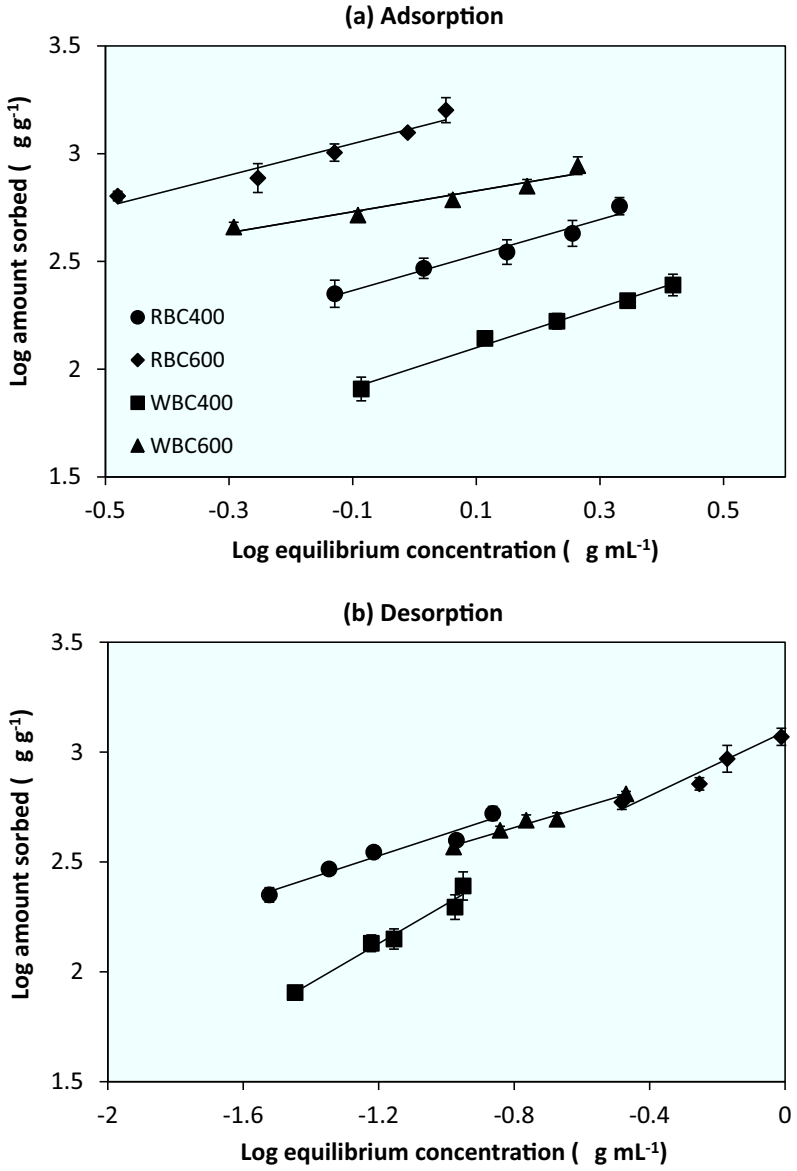

Fig. 2 Adsorption (a) and desorption (b) isotherms for pyrazosulfuron-ethyl in non-deashed biochars.

adsorption equation satisfactorily explained the sorption of pyrazosulfuron-ethyl in biochars and the results were significant at 99% levels.

The slope (1/n) values for pyrazosulfuron-ethyl adsorption isotherms in both normal and deashed biochars were < 1 indicating nonlinear adsorption isotherms. The slope value < 1 suggested L-type adsorption isotherms which are obtained when molecules are sorbed in a flat position, not suffering a strong competition from water molecules. This explains the high affinity to the sorbent for solutes at low concentrations. However, as the concentration the sorption sites become limited and sorption (Zhou et al., 2013; Liu et al., 2015; Mayakaduwa et al., 2015). Nonlinearity in pyrazosulfuron-ethyl adsorption increased with increase in the pyrolysis temperature. Sun et al. (2013) suggested that increase in isotherm nonlinearity with increasing biochar pyrolysis temperature can be attributed to higher aromaticity of these biochars. Higher microporosity of high temperature biochars might contribute to greater nonlinearly of isotherms (Chefetz and Xing, 2009). Furthermore, deashing of biochars increased the isotherm nonlinearity as 1/n values varied from 0.61–0.93 in normal biochars and 0.39–0.57 in deashed biochars. Increased isotherm nonlinearity in deashed biochars can be attributed to higher surface area, microporosity and aromaticity (Chun et al., 2004; Chefetz and Xing, 2009). A significant correlation between nonlinearity parameter (1/n) and total carbon content ($r = -0.827$, $p = 0.05$), organic carbon content ($r = -0.866$, $p = 0.05$) and O/C ratio (polarity) ($r = 0.907$, $p = 0.05$) of biochars was observed suggesting that nonlinearlity increased with increase in TC/TOC and decrease in polarity. Increase in nonlinearity when pH decreased from alkaline (normal biochar) to acidic (deashed biochar) suggested that different pyrazosulfuron species at different pH ($pK_a - 3.7$).

The Freundlich sorption constants (K_f) for pyrazosulfuron-ethyl for normal biochars were higher in biochars prepared at 600 °C (601.17 and 1317.31 $\mu g^{(1-1/n)}$ g^{-1} $mL^{1/n}$ for WBC600

and RBC600, respectively) than for those prepared at 400 °C (101.48 and 280.29 $\mu g^{(1-1/n)}\ g^{-1}\ mL^{1/n}$ for WBC400 and RBC400, resp.) Deashing of biochars further increased the K_f values and respective values in deashed biochars were 294.71 (WBC400d), 1137.1 (WBC600d), 758.01 (RBC400d) and 4227.1 $\mu g^{(1-1/n)}\ g^{-1}\ mL^{1/n}$ (RBC600d). The maximum increase was observed in the RBC600d (3.21 times) and was followed by WBC400d (2.90 times), RBC400d (2.7 times) and WBC600d (1.89 times). Increased herbicide adsorption in deashed biochars can be attributed to higher surface area and porosity following removal of the mineral fraction.

The K_{oc} (organic carbon normalized adsorption coefficient, $K_{oc} = K_f$ X 100/Percent OC content) values of pyrazosulfuron-ethyl sorption were higher for rice biochars than wheat biochars. Furthermore, the K_{oc} values increased with increasing pyrolysis temperature. These results were in opposition to those reported by Sun et al. (2011) who suggested that low temperature biochars have more polar groups and therefore, provide more adsorption sites for norflurazon and fluridone sorption via specific adsorption sites. The K_{oc} values in the present study increased after deashing of biochars as removal of the mineral fraction resulted in an increase in surface area and sorption of pyrazosulfuron increased. Furthermore, acid treatment might have resulted in increase in functional groups which could provide additional sites for pyrazosulfuron-ethyl sorption (Taha et al., 2014).

The results of pyrazosulfuron-ethyl desorption from normal and deashed biochars during are presented in Table 3. Results showed that 0.6–5.2, 19–29.8, 0–7.88 and 6.92–7.78% of pyrazosulfuron-ethyl were desorbed from WBC400, WBC600, RBC400 and RBC600 biochars, respectively. Thus, more herbicide desorption was observed from non-deashed high temperature (600 °C) biochars than from biochars prepared at 400 °C. Rice biochars retained a higher percentage of sorbed pyrazosulfuron-ethyl than the wheat biochars. Maximum herbicide desorption was observed from the WBC600 while RBC400 was the best biochar to retain sorbed pyrazosulfuron-ethyl. In general, higher amounts of pyrazosulfuron-ethyl were desorbed from the deashed counterparts and 5.79–12.09%, 20.49–41.37%, 11.88–21.01% and 3.68–15.69% herbicide desorption was observed from WBC400d, WBC600d, RBC400d and RBC600d biochars, respectively. No report on desorption behavior of contaminants in deashed biochar is available.

Pyrazosulfuron-ethyl desorption data from normal and deashed biochars was subjected to the Freundlich equation and results are shown in Fig. 3 and Table 3. The $1/n_{des}$ values were lower than the corresponding $1/n_{ads}$ values suggesting that rate of desorption was lower than the rate of adsorption and hysteresis was observed. The hysteresis ($H = 1/n_{des}/1/n_{ads}$) is negative when H is >1 and positive when the H is <1. Generally, desorption of pyrazosulfuron-ethyl biochars showed positive hysteresis. Moreover, slope values for pyrazosulfuron-ethyl desorption from deashed biochars showed higher nonlinearity than those from normal biochars. Except for RCB600d the K_f values for pyrazosulfuron-ethyl desorption from deashed biochars were higher in low temperature biochars and can be explained by lower herbicide desorption from biochars prepared at 400 °C.

The change in free energy (ΔG) for pyrazosulfuron-ethyl sorption via biochars was calculated using following equation:

$$\Delta G = -RT\ \ln\ K_{eq}$$

ΔG is the free energy change (kcal mol^{-1}), R is the gas constant (1.986 cal $K^{-1}\ mol^{-1}$), T is the absolute temperature in K and Keq is the thermodynamic equilibrium constant and was calculated from K_f by method suggested by Ghosal and Gupta (2015). The ΔG is used as a measure of the extent of the driving force in the adsorption process. The greater the absolute magnitude of ΔG, the greater is the extent to which the adsorption reaction may take place. Negative ΔG values suggested that the process exothermic and spontaneous. In general, the ΔG values were higher in rice biochars than wheat biochars and deashed biochars showed higher values than normal biochars with the exception of WBC600 where WBC600d had higher change in free energy (Table 4).

To study the mechanism of pyrazosulfuron-ethyl adsorption on normal biochars, the FTIR spectra of pure pyrazosulfuron-ethyl, biochar and biochar-pyrazosulfuron-ethyl (PE) interaction complexes were analyzed (Fig. 4). Comparison of biochar and biochar-pyrazosulfuron-ethyl complex spectra suggested that few additional peaks appeared in the interaction product spectra while the intensities of prominent biochar signals changed significantly. Absorbance at 3434 cm^{-1} (O—H stretching) was significantly reduced in WBC600-PE (T = 47% to T = 16%) interaction products. The observations for the signal at 1629 cm^{-1} (C═C stretching of aromatic components and C═O stretching in quinones and ketonic acids) were similar. However, a weak band in the 1250–1100 cm^{-1} region, which can be assigned to the C—O stretching/O—H deformation vibration and Si-O stretching, significantly increased in the interaction product. These results suggested that phenolic or alcoholic groups in biochar can

Table 3 Freundlich parameters for pyrazosulfuron-ethyl desorption in biochars.

Treatment	K_f	1/n	r	Amount desorbed [%]
WBC400	1615.1	0.90	0.987	0.6–5.2
WBC600	1051.5	0.46	0.987	19.0–29.8
RBC400	1357.7	0.50	0.972	0.0–7.9
RBC600	1240.8	0.73	0.973	6.9–7.8
WBC400d	1031.8	0.47	0.957	5.8–12.1
WBC600d	791.0	0.22	0.994	20.5–41.4
RBC400d	1309.2	0.46	0.988	11.9–21.0
RBC600d	3013.0	0.34	0.974	3.7–9.7

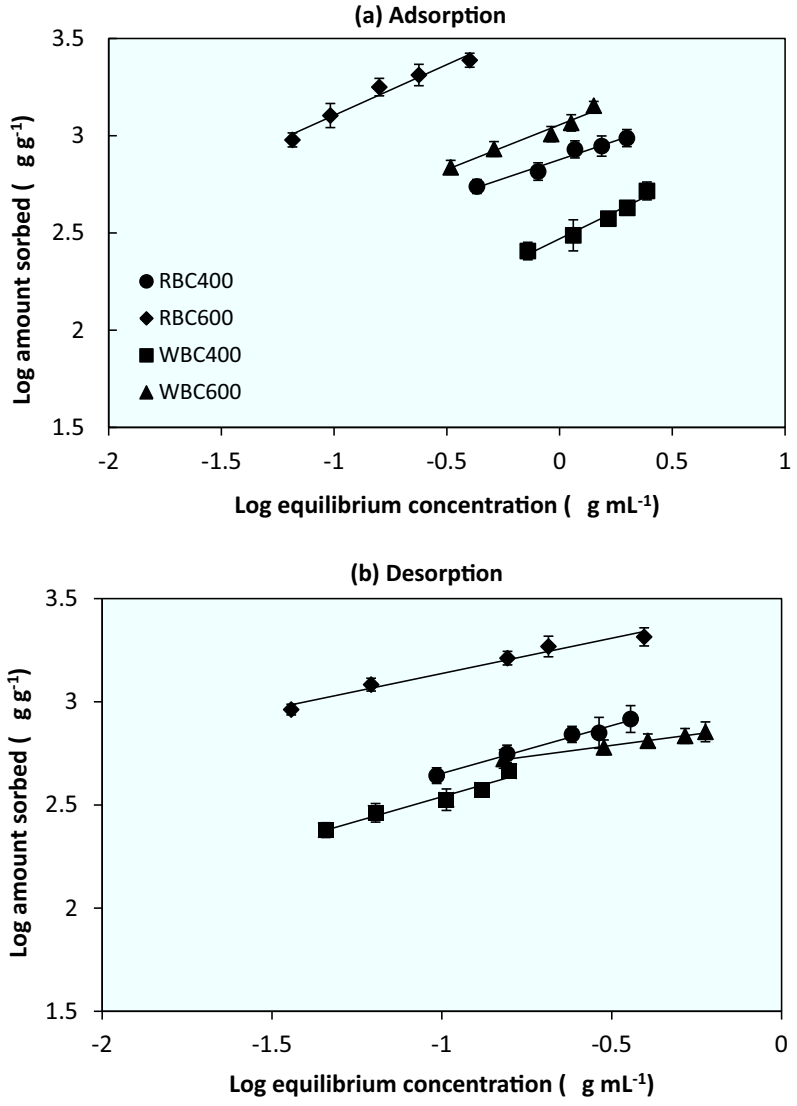

Fig. 3 Adsorption (a) and desorption (b) isotherms for pyrazosulfuron-ethyl in deashed biochars.

form H-bonds with herbicide molecule. The interaction product showed two additional signals at ~1500 and 1420 cm^{-1} which can be assigned to C=N stretching vibration in pyrazosulfuron-ethyl bound to biochar.

The effect of physico-chemical properties of biochars on pyrazosulfuron-ethyl adsorption was evaluated using K_f as adsorption parameter. Results of correlation (Table 5, Fig. 5) study suggested that values of correlation coefficient (r) varied with nature of biochar; probably, acid treatment affected the chemical characteristics of biochars. The pyrazosulfuron-ethyl adsorption on normal biochars correlated with biochar's pH (r = −0.996, P = .01), porosity (r = 0.947, P = 0.01), total carbon (r = 0.921, P = 0.1) and total organic carbon (r = 0.939, P = 0.1) content; while, deashed biochars showed significant correlation with biochar's pH (r = −0.959, P = 0.05), surface area (r = 0.969, P = 0.05) and porosity (r = 0.995, P = 0.01). Earlier studies have suggested that sorption of sulfonylurea herbicides was negatively correlated to the substrate pH (Pusino et al., 2003; Zhang and Wang, 2007; Singh and Singh, 2012). Pyrazosulfuron-ethyl adsorption on biochars did not show significant correlation with aromaticity [H/C ratio; r-0.776 (normal); r-0.706 (deashed)]. Probably, it is not the total aromatic content, but the nature of aromatic fraction which affected the herbicide adsorption. Negative correlation between adsorption and O/C ratio (polarity index) of the biochars suggested that pesticide adsorption was affected by degree of biochar's polarity and herbicide was preferentially sorbed on the nonpolar sites (aliphatic and aromatic component) in biochars. This was further confirmed by increase in herbicide adsorption in deashed biochars which were less polar than the normal biochars. Earlier, Huang and Chen (2010) suggested that organic carbon fraction of ash charcoal have different functionalities for sorption which operates by "adsorption" and "partitioning" phenomenon. They suggested that relative contribution of "adsorption" to total sorption of polar solutes was higher than

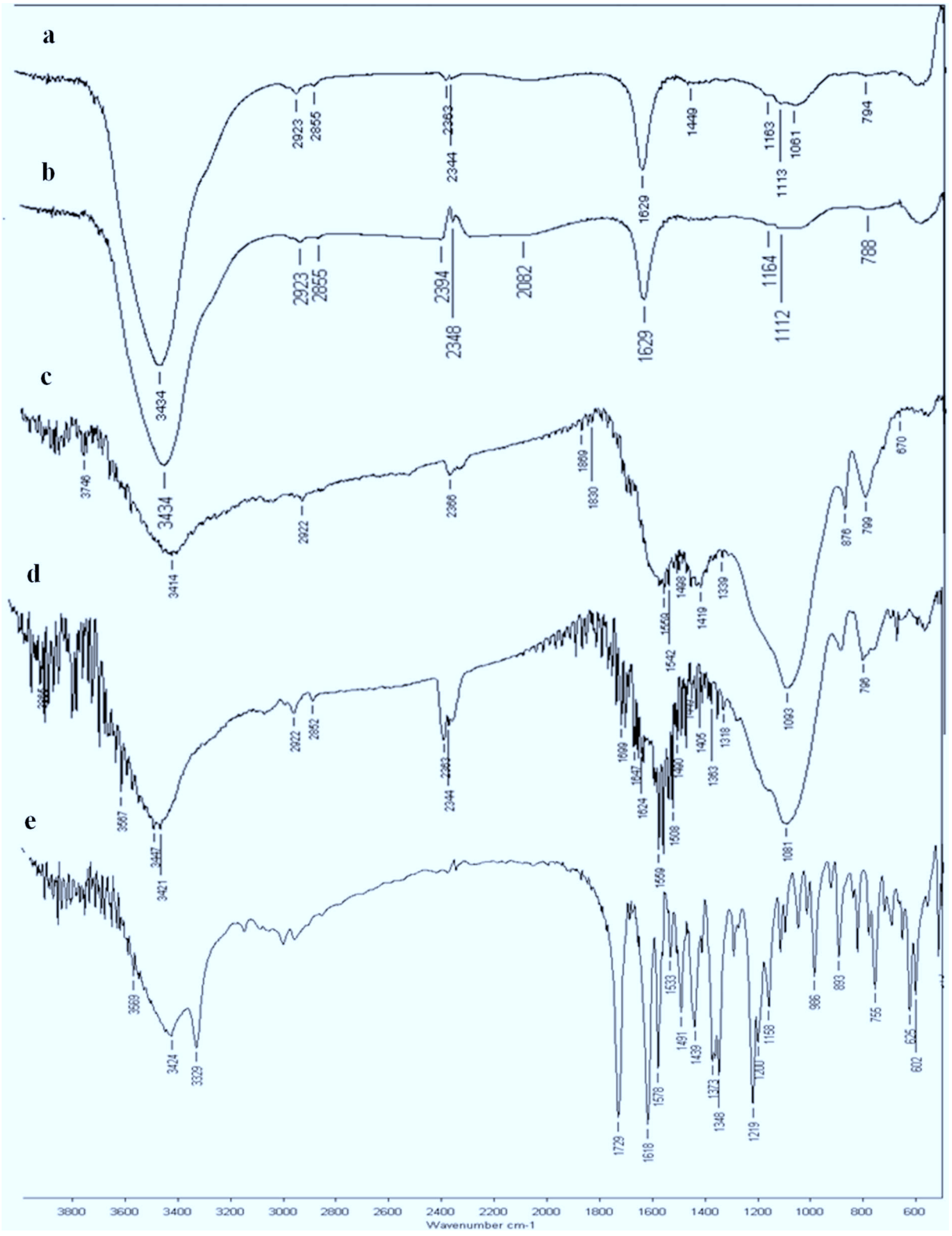

Fig. 4 FTIR spectra of (a) RBC600 (b) WBC600 (c) Pyrazosulfuron-RBC600 (d) Pyrazosulfuron-WBC600 and (e) Pyrazosulfuron-ethyl.

Table 4 Free energy change (ΔG) values for the adsorption of pyrazosulfuron-ethyl in biochars.

Treatment	ΔG (T = 27 °C) [kcal mol^{-1}]
WBC400	−98.077
WBC600	−5298.1
RBC400	−579.06
RBC600	−4729.1
WBC400d	−3423.6
WBC600d	−28242
RBC400d	−30533
RBC600d	−69375

"partition" in normal ash charcoal; but, contribution of "adsorption to sorption decreased and "partition" increased in deashed charcoal. They suggested that the acid treatment changed some properties and/or some structures of charcoal.

4. Conclusion

The study suggested that sorption of pyrazosulfuron-ethyl on biochars was greatly affected by the pyrolysis temperature and rice biochars were more effective than the corresponding wheat biochars in adsorbing pyrazosulfuron-ethyl. Herbicide adsorption was nonlinear and decreased with increasing concentration. Deashing of biochars significantly increased their herbicide sorption potential, but nonlinearity increased significantly. Nonlinearity was mainly attributed to total carbon, total organic carbon and polarity index. Biochar's surface area, pore volume and pH significantly contributed to pyrazosulfuron-ethyl sorption potential. Results of this study suggested that the mineral fraction of biochars significantly affected pyrazosulfuron-ethyl sorption. It will help in predicting the sorption properties of biochar-amended soils and better understanding the degradation and mobility of herbicide in soil amended with biochar.

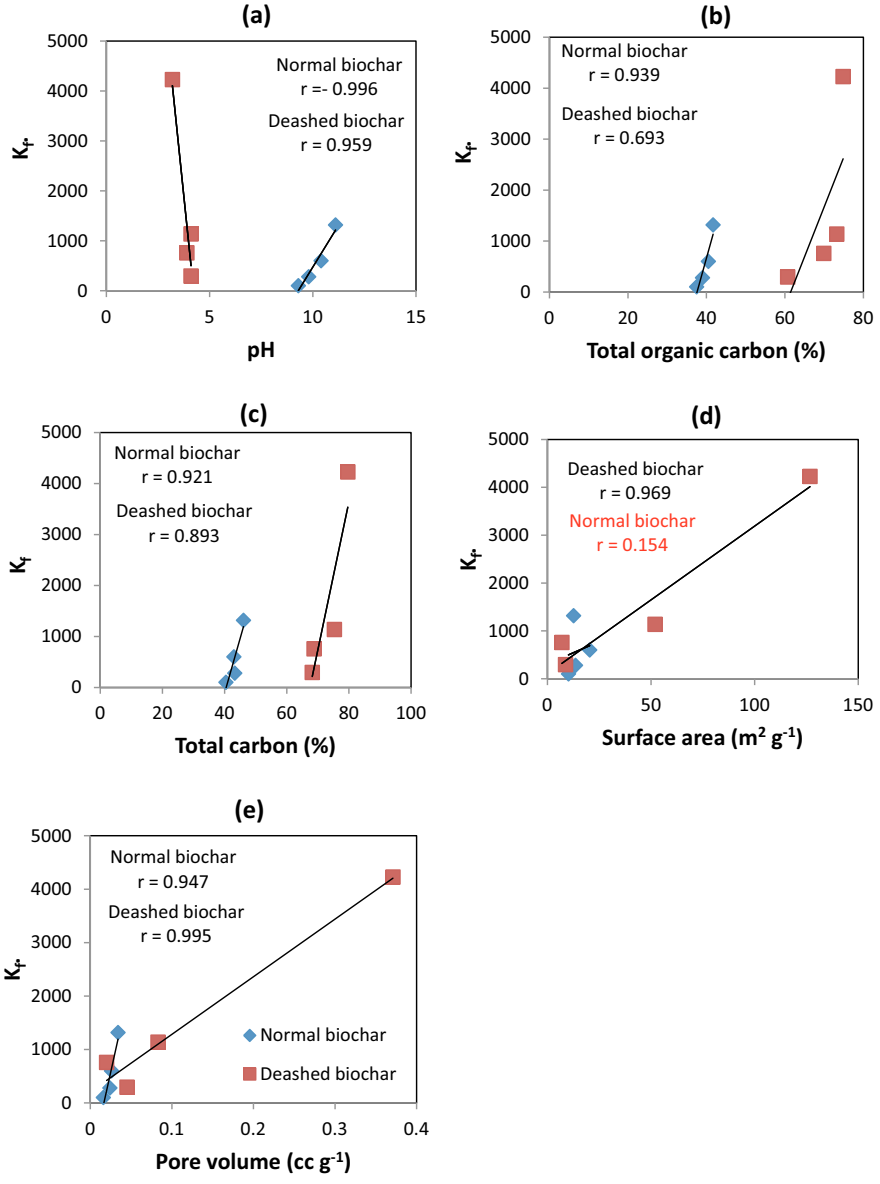

Fig. 5 Correlation of Freundlich adsorption parameter (K_f) with physico-chemical properties of biochar.

Table 5 Pearson correlation coefficients (r) and significance of linear relationship between physico-chemical properties of biochars and pyrazosulfuron-ethyl adsorption parameter (K_f).

Factors	Normal biochars		Deashed biochars		Both biochars	
	r	Significance	r	Significance	r	Significance
% C	0.921	*	0.893	NS	0.593	NS
% O	0.830	NS	0.508	NS	0.552	NS
H/C	−0.776	NS	−0.706	NS	−0.639	*
O/C	−0.846	NS	−0.572	NS	−0.550	NS
% TOC	0.939	*	0.693	NS	0.566	NS
Surface area ($m^2\ g^{-1}$)	0.154	NS	0.969	**	0.942	****
Porosity ($cm^3\ g^{-1}$)	0.947	*	0.995	**	0.966	****
pH	−0.996	***	0.959	**	−0.392	NS

NS = non-significant.
* Significance at < 0.1.
** Significance at < 0.05.
*** Significance at < 0.01.
**** Significance at < 0.001.

Appendix A. Supplementary material

Supplementary data associated with this article can be found, in the online version, at https://doi.org/10.1016/j.arabjc.2017.10.005.

References

Cabrera, A., Cox, L., Spokas, K.A., Hermosín, M.C., Cornejo, J., Koskinen, W.C., 2014. Influence of biochar amendments on the sorption–desorption of aminocyclopyrachlor, bentazone and pyraclostrobin pesticides to an agricultural soil. Sci. Total Environ. 470–471, 438–443.

Chefetz, B., Xing, B., 2009. Relative role of aliphatic and aromatic moieties as sorption domains for organic compounds: a review. Environ. Sci. Technol. 43, 1680–1688.

Chun, Y., Sheng, G., Chiou, C.T., Xing, B., 2004. Composition and sorptive properties of crop residue-derived chars. Environ. Sci. Technol. 38, 4649–4655.

Cornelissen, G., Gustafsson, Ö., Bucheli, T.D., Jonker, M.T., Koelmans, A.A., van Noort, P.C., 2005. Extensive sorption of organic compounds to black carbon, coal, and kerogen in sediments and soils: Mechanisms and consequences for distribution, bioaccumulation, and biodegradation. Environ. Sci. Technol. 39, 6881–6895.

Gamiz, B., Velarde, P., Spokas, K.A., Hermosin, M.C., Cox, L., 2017. Biochar soil additions affect herbicide fate: importance of application timing and feedstock species. J. Agric. Food Chem. 65, 3109–3117.

Ghosal, P.S., Gupta, A.K., 2015. An insight into thermodynamics of adsorptive removal of fluoride by calcined Ca–Al–(NO_3) layered double hydroxide. RSC Adv. 5, 105889–105900.

Huang, W., Chen, B., 2010. Interaction mechanism of organic contaminants with burned straw ash charcoal. J. Environ. Sci. 22, 1586–1594.

Jackson, M.L., 1967. Soil Chemical Analysis. Prentice Hall Inc., New Delhi, India.

Jain, N., Bhatia, A., Pathak, H., 2014. Emission of air pollutants from crop residue burning in India. Aerosol Air Qual. Res. 14, 422–430.

Keiluweit, M., Nico, P.S., Johnson, M.G., Kleber, M., 2010. Dynamic molecular structure of plant biomass-derived black carbon (biochar). Environ. Sci. Technol. 44, 1247–1253.

Kolodynska, D., Wnetrzak, R., Leahy, J.J., Hayes, M.H.B., Kwapinski, W., Hubicki, Z., 2012. Kinetic and adsorptive characterization of biochar in metal ions removal. Chem. Eng. J. 197, 295–305.

Liu, N., Charrua, A.B., Weng, C.H., Yuan, X., Ding, F., 2015. Characterization of biochars derived from agriculture wastes and their adsorptive removal of atrazine from aqueous solution: a comparative study. Bioresour. Technol. 198, 55–62.

Mandal, A., Singh, N., Purakayastha, T.J., 2017. Characterization of pesticide sorption behaviour of slow pyrolysis biochars as low cost adsorbent for atrazine and imidacloprid removal. Sci. Total. Environ. 577, 376–385.

Mayakaduwa, S., Kumarathilaka, P., Herath, I., Ahmad, M., Al-Wabel, M., Ok, Y.S., Usman, A., Abduljabbar, A., Vithanage, M., 2015. Equilibrium and kinetic mechanisms of woody biochar on aqueous glyphosate removal. Chemosphere 144, 2516–2521.

Mukome, F.N.D., Zhang, X., Silva, L.C.R., Six, J., Parikh, S.J., 2013. Use of chemical and physical characteristics to investigate trends in biochar feedstocks. J. Agric. Food Chem. 61, 2196–2204.

Pandian, K., Subramanianyan, P., Gnasekaran, P., Chitraputhirapillai, S., 2016. Effect of biochar amendment on soil physical, chemical and biological properties and groundnut yield in rainfed Alfisol of semi-arid tropics. Arch. Agron. Soil Sci. 62, 1293–1310.

Pastorova, I., Botto, R.E., Arisz, P.W., Boon, J.J., 1994. Cellulose char structure: a combined analytical Py-GC-MS, FTIR, and NMR study. Carbohydr. Res. 262, 27–47.

Peng, X., Liu, X., Zhou, Y., Peng, B., Tang, L., Luo, L., Yao, B., Deng, Y., Tang, J., Zeng, G., 2017. New insights into the activity of a biochar supported nanoscale zerovalent iron composite and nanoscale zero valent iron under anaerobic or aerobic conditions. RSC Adv. 7, 8755–8761.

Pusino, A., Fiori, M.G., Braschi, I., Gessa, C., 2003. Adsorption and desorption of triasulfuron by soil. J. Agric. Food Chem. 51, 5350–5354.

Rajapaksha, A.U., Vithanage, M., Zhang, M., Ahmad, M., Mohan, D., Chang, S.X., Ok, Y.S., 2014. Pyrolysis condition affected sulfamethazine sorption by tea waste biochars. Bioresour. Technol. 166, 303–308.

Singh, N., Singh, S.B., 2012. Sorption-desorption behavior of metsulfuron-methyl and sulfosulfuron in soils. J. Environ. Sci. Health B 47, 168–174.

Sohi, S., Krull, E., Lopez-Capel, E., Bol, R., 2010. A review of biochar and its use and function in soil. Adv. Agron. 105, 47–82.

Sun, K., Keiluweit, M., Kleber, M., Pan, Z., Xing, B., 2011. Sorption of fluorinated herbicides to plant biomass-derived biochars as a function of molecular structure. Bioresour. Technol. 102, 9897–9903.

Sun, K., Kang, M., Zhang, Z., Jin, J., Wang, Z., Pan, Z., Xu, D., Wu, F., Xing, B., 2013. Impact of deashing treatment on biochar

structural properties and potential sorption mechanisms of phenanthrene. Environ. Sci. Technol. 47, 11473–11481.

Taha, S.M., Amer, M.E., Elmarsafy, A.E., Elkady, M.Y., 2014. Adsorption of 15 different pesticides on untreated and phosphoric acid treated biochar and charcoal from water. J. Environ Chem. Eng. 2, 2013–2025.

Wang, T.T., Cheng, J., Liu, X.J., Jiang, W., Zhang, C.L., Yu, X.Y., 2012. Effect of biochar amendment on the bioavailability of pesticide chlorantraniliprole in soil to earthworm. Ecotoxicol. Environ. Saf. 83, 96–101.

Wu, W., Yang, M., Feng, O., McGrouther, K., Wang, H., Lu, H., Chen, Y., 2012. Chemical characterization of rice straw-derived biochar for soil amendment. Biomass Bioenergy 47, 268–276.

Yang, F., Cao, X., Gao, B., Zhao, L., Li, F., 2015. Short-term effects of rice straw biochar on sorption, emission, and transformation of soil NH_4^+-N. Environ. Sci. Pollut. Res. 22, 184–9192.

Yang, X.B., Ying, G.G., Peng, P.A., Wang, L., Zhao, J.L., Zhang, L. J., Yuan, P., He, H.P., 2010. Influence of biochars on plant uptake and dissipation of two pesticides in an agricultural soil. J. Agric. Food Chem. 58, 7915–7921.

Yavari, S., Malakahmad, A., Sapari, N.B., 2015. Biochar efficiency in pesticides sorption as a function of production variables—a review. Environ. Sci. Pollut. Res. 22, 13824–13841.

Yu, F., Sun, L., Zhou, Y., Gao, B., Gao, W., Bao, C., Feng, C., Li, Y., 2016. Biosorbents based on agricultural wastes for ionic liquid removal: An approach to agricultural wastes management. Chemosphere 165, 94–99.

Zhang, J., Liu, J., Liu, R., 2015. Effect of pyrolysis temperature and heating time on biochar obtained from the pyrolysis of straw and lignosulfonate. Bioresour. Technol. 176, 288–291.

Zhang, P., Sun, H., Yu, L., Sun, T., 2013. Adsorption and catalytic hydrolysis of carbaryl and atrazine on pig manure-derived biochars: impact of structural properties of biochars. J. Hazard. Mat. 244–245, 217–224.

Zhang, W., Wang, J.J., 2007. Effect of solution pH and simulated acid rain on the behaviour of two sulfonyl urea herbicides in soil. Ying Yong Sheng Tai Xue Bao 18, 613–619.

Zhou, Y.M., Gao, B., Zimmerman, A.R., Fang, I., San, Y.N., Gao, X. D., 2013. Sorption of heavy metals on chitosan-modified biochars and its biological effects. Chem. Eng. J. 231, 512–518.

Zhou, Y., Liu, X., Xiang, Y., Wang, P., Zhang, J., Zhang, F., Wei, J., Luo, L., Leia, M., Tang, L., 2017b. Modification of biochar derived from sawdust and its application in removal of tetracycline and copper from aqueous solution: adsorption mechanism and modelling. Bioresour. Technol. 245, 266–273.

Zhou, Y., Liu, X., Tang, L., Zhang, F., Zeng, G., Peng, X., Luo, L., Deng, Y., Pang, Y., Zhang, J., 2017a. Insight into highly efficient co-removal of *p*-nitrophenol and lead by nitrogen-functionalized magnetic ordered mesoporous carbon: Performance and modelling. J. Hazard. Mat. 333, 80–87.

Zhou, Z., Shi, D., Qiu, Y., Sheng, G.D., 2010. Sorptive domains of pine chars as probed by benzene and nitrobenzene. Environ. Pollut. 158, 201–206.